Size Effect on Shear Strength of RC Deep Beams Strengthened with Carbon Fiber Reinforced Polymer (CFRP)

Walat Omer Miro[1] & Bahman Omer Taha[2] & Kamaran S. Ismail[3]

[1&3]Civil Engineering Department, Faculty of Engineering, Soran University, Soran, Kurdistan Region, Iraq
[2]Department of Civil Engineering, Erbil Technical Engineering College, Erbil Polytechnic University, Erbil, Iraq
Correspondence: Walat Omer Miro, Civil Engineering Department, Faculty of Engineering, Soran University, Soran, Kurdistan Region, Iraq.
Email: walatomercivil@gmail.com

Doi: 10.23918/eajse.v8i3p122

Abstract: When the size of a conventional reinforced concrete deep beam is increased, the shear strength of the concrete at failure decreased. This is called the "size effect." However, there has been very little research on the size effect in reinforced concrete (RC) deep beams strengthened using carbon fiber-reinforced polymer (CFRP) u-strip. This study examines how shear strengthening with CFRP strips affects the size effect. Six RC deep beams with the same shear span depth ratio (a/d=1.5) and width (b=150mm) are tested. The investigated parameters were beam height and strengthening with CFRP. The results showed that, the shear strength of the deep beams strengthened with CFRP u-strips increased by about 12–50% in comparison to the comparable control beams. CFRP may influence the size effect of shear strengthened deep beams, as the loss in ultimate shear strength was lowered from 76% to 32% when the height was increased from 200 mm to 600 mm. In addition, the presence of CFRP increased diagonal cracking strength on unstrengthened specimens by 47%, 46.8%, and 55% for 200mm, 400mm, and 600mm specimens, respectively.

Keyword: Deep Beams, Size Effect, CFRP, Shear Strength

1. Introduction

A deep beam is a member that is loaded on one side and supported on the other, with clear spans that are less than four times the depth of the member, or with areas of concentrated loads (shear span) that are no more than half the depth of the member away from the face of the support. (Committee, 2019). There are several uses for deep beams in the construction of such as transfer girder in tall buildings, foundations and offshore structures. In most cases, deep beams are transfer girders that carry the weight of one or more columns and transmit it laterally to other columns, and the safety of the whole structure depends on the safety of the deep beams. Therefore, the safety margin for designing RC deep beams must be accurately predicted. However, many structures built according to earlier design regulations may be structurally unstable. Rebuilding damaged or structurally unsafe buildings would demand a major public investment of money and effort. Strengthening RC components has emerged as a feasible alternative technique because of its potential to increase load-bearing capacity while maintaining service life. (Saribiyik, Abodan and Balci, 2021)

In civil infrastructure, FRP materials are being used to upgrade reinforced concrete structures and create new structures.

Received: October 1, 2021
Accepted: December 12, 2022
Miro, W.O., & Taha, B.O., & Ismail, K.S. (2022). Size Effect on Shear Strength of RC Deep Beams Strengthened with Carbon Fiber Reinforced Polymer (CFRP). *Eurasian Journal of Science and Engineering, 8*(3),122-138.

Attaching FRP plates or sheets externally to corroded structural components increases their shear strength. (Kim, Sim, and Oh, 2008). The extensive use of FRP in civil engineering might lead to size effect difficulties. Much research has examined the shear strength of FRP-reinforced RC deep beams, but few have evaluated size. (Qu and Lu, 2005)

As has been demonstrated by a number of experimental studies, the shear strength (V/bd) of RC beams decreases as beam size increases (this phenomenon is known as the "size effect"). (Kani, 1967; Bazant, 1991; Ghannoum, 1998; Syroka-Korol and Tejchman, 2014; El-Sayed and Shuraim, 2016). The decrease in aggregate interlock and residual tensile strength may cause this phenomenon if the spacing and width of fractures grow together with the effective depth of the beam. (Jumaa and Yousif, 2019)

Several criteria impact the behavior of reinforced concrete elements strengthened under shear with external FRP stirrups. Unquestionably, the size of the beam is one of the most crucial elements influencing the final capacity of a shear-reinforced beam. The size effect is particularly important in the context of FRP-reinforced beams because it establishes the connection between the effective bond length and the effective FRP strain, and hence the shear capacity. (Khalifa and Nanni, 2000; Deniaud and Cheng, 2001). Despite this, few studies have been published on the size effect in RC beams reinforced by U-shaped or totally wrapped strip CFRP. (Leung et al., 2007; Godat et al., 2010). However, only a few researchers have explored the size effect of FRP-shear-reinforced RC beams. (Deniaud and Cheng, 2001; Qu and Lu, 2005; Leung et al., 2007; Bae et al., 2012; Nguyen-Minh, , and M. Rovňák, 2015;Foster et al., 2017; Benzeguir et al., 2019). According to (Triantafillou and Antonopoulos, 2000), There should be a correlation between beam size and the FRP contribution to shear resistance, as a bigger beam size provides more bonding surface for FRPs. (Leung et al., 2007) rectangular RC beams were subjected to testing using U-wrap and full-wrap schemes with steel stirrups and EB-CFRP strips. The total shear strength of U-wrap-enhanced specimens decreased by 50% as a result of their increased size. There was no effect on size from using full-wrap specimens. (Godat et al., 2010) investigated the shear strengthening properties of U-wrapped EB-CFRP strips on rectangular RC beams devoid of steel stirrups. Researchers found that shear resistance of FRP was independent of its size. (Qu and Lu, 2005) examined the shear strengthening effects of U-wrapped EB-CFRP strips on three different sized rectangular RC beams. According to the findings of the study, the size does not affect the shear resistance of FRP. (Foster et al., 2017) investigated the size effect on RC T-beams with internal transverse steel that were reinforced in shear with continuous EB-CFRP sheets, by adopting a U-wrap technique that included a near-surface-mounted bar-in-slot on the web. The shear strength was reduced by 24% when bigger beams were used.

This experimental research endeavors to evaluate the size effect in shear-strengthened RC deep beams using carbon fiber reinforced plastic (CFRP) strips. The purpose of this research is twofold: first, To Evaluate and investigate the effect of beam height on the shear strength response of RC deep beams, and second, to analyze the effect of shear strengthening using CFRP u-shaped strips on the size effect of RC deep beams.

2. Experimental Program

2.1 Test Specimens

The experimental program of the current research study consists of casting and testing six RC deep beams under three points bending. Figure 1. depicts the geometrical dimensions and reinforcing details for all beams. The nominal shear span-to-depth ratio a/d was 1.5 for all the beams; and all the beams

had the same width, which had 150mm; the span L was raised proportionately with the height h of the beams; and with three different heights: small size specimens

with 200mm height, medium size specimens with 400 mm height, and large size specimens with 600 mm height and had clear covers of 20 mm. A total of two sets of tested beams were created. Different height sizes of a beam were made available for the three beams in series one (1-W4-100, 2-W2-100, 3-W5-100) that were not strengthened with CFRP. In series two (4-W9-CFRP-100, 5-W7-CFRP-100, and 6-W10-CFRP-100), the same dimensions were supplied to the beams that were strengthened with CFRP.

As the longitudinal tensile reinforcement, steel rebars with diameters of 8, 10, 12, 16, and 20 mm were employed. Small size specimens, 200 mm in height, involve 2 Ø 16 and 1 Ø 8 for tension reinforcement, placed in a single layer with their centroid located at a depth of 166 mm from the top surface of the beam, while medium size specimens, 400 mm in height, involve 4 Ø 16 and 2 Ø 10, placed in a pair of layers with their centroid located at a depth of 346 mm. Finally, large-size specimens, 600 mm in height, involve 4 Ø 20 and 2 Ø12 This steel reinforcement layout ensures that shear failure, rather than flexural failure, will control the beam's ultimate capacity. All beams have 2 Ø 10 web reinforcement, with the top steel bars functioning as hangers. All beams had their minimum shear reinforcement (horizontal and vertical) installed with 6 mm diameter vertical steel placed at 130 mm on center for all specimens and 4,6 mm diameter horizontal steel placed at 61 mm, 140 mm, and 140 mm on center for small, medium, and large specimens, respectively. Minimum vertical and horizontal shear reinforcement (ρ_v=0.28%, ρ_h=0.27%). was given for all beams, and the flexural reinforcement ratio was held constant across all specimens at =1.82%. Table 1. Provides a summary of the specimen sizes and longitudinal steel quantities for each beam.

Table 1: Properties of tested beams

Group no.	Specimen symbol	Total length mm	Clear span mm	b mm	h mm	d mm	a mm	a/d	ρ	ρ_v	ρ_h	Bp	CFRP
G1	1-W4-100	800	498	150	200	166	249	1.5	0.0182	0.0028	0.0027	100	Nil
	2-W2-100	1400	1038		400	346	519	1.5	0.0182	0.0028	0.0027	100	Nil
	3-W5-100	2000	1626		600	542	813	1.5	0.0182	0.0028	0.0027	100	Nil

G2	4-W9-CFRP-100	800	498	150	200	166	249	1.5	0.0182	0.0028	0.0027	100	CFRP
	5-W7-CFRP-100	1400	1038		400	346	519	1.5	0.0182	0.0028	0.0027	100	CFRP
	6-W10-CFRP-100	2000	1626		600	542	813	1.5	0.0182	0.0028	0.0027	100	CFRP

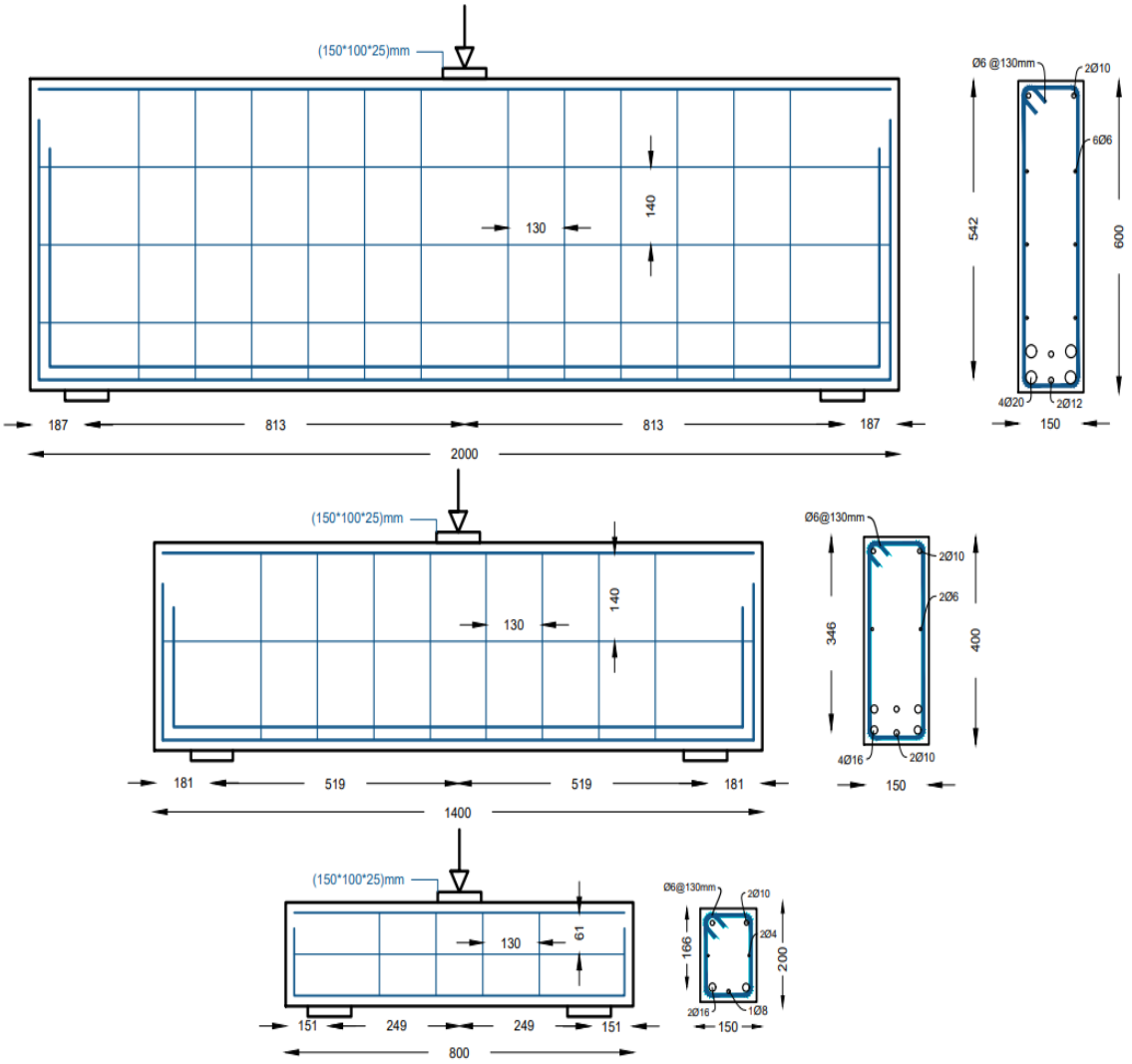

Figure 1: Dimensions and reinforcement details of Specimens

2.2 Material Properties

All of the beams were cast in a plywood mold and cured for 10 days in the same environment before the mold was removed. There were two different batches: one for beams that hadn't been strengthened (group 1) and the other for beams that had been strengthened (Group 2). Compressive strength f_{cu} was determined by casting six typical concrete cubes with dimensions of 150mm x 150mm x 150mm according to Eurocode EN 12390-3(Eurocode EN, 2009), and the equivalent cylinder strength, denoted by the symbol f'_c, was determined to be 0.85% of the cube strength. (Ashour, 1997). While the concrete splitting tensile strength (f_{ct}) was determined by testing a cylinder of standard size (100 mm by 200 mm) concrete according to ASTM C496 (ASTM C496, 1996). The average concrete strength and splitting tensile strength at 65 days were therefore different for strengthened and unreinforced beams. Unstrengthened beams (G1) had average compressive concrete strengths f'_c of 41.2 MPa and splitting tensile strengths f_{ct} of 2.88 MPa, whereas strengthened beams (G2) saw these values drop to 32.98 MPa and 2.5 MPa, respectively.

Table 2. Displays the typical mechanical characteristics of longitudinal and transverse steel bars. Three specimens were averaged to determine the yield strengths (575 MPa, 594 MPa, 616 MPa, 441 MPa, 473 MPa, and 678 MPa for 20 mm, 16 mm, 12 mm, 10 mm, 8 mm, 6 mm, and 4 mm diameters, respectively, following ASTM A370-19. (ASTM-A370-19, 2019)

For strengthening purposes, an FRP system that is already on the market (Sika Wrap Hex®) had been chosen. Manufacturer claims for CFRP sheet (SikaWrap®-300 C) include an average of 4000 MPa (average tensile strength), 23 GPa (average longitudinal elastic modulus), and 1.7% ultimate strain. According to the manufacturer's instructions, an epoxy adhesive (Sikadur® 330) with 4.5 GPa elasticity modulus, 30 MPa ultimate tensile strength, and 0.9% ultimate strain was used to connect the CFRP to the concrete. In table 3, the mechanical characteristics of the CFRP sheet were shown.

Table 2: Mechanical Properties of Steel Reinforcement

Mechanical property	Steel stirrup		Longitudinal steel reinforcement				
	Ø4	Ø6	Ø8	Ø10	Ø12	Ø16	Ø20
Area mm^2	12	28	50	78	113	201	314
Yield strength f_y,MPa	678	733	473	441	616	594	575
ultimate strength f_u,MPa	862	787	671	685	726	723	742

Table 3. Mechanical Properties of CFRP Sheet

Property	Specification	Test method
Area weight (g/m^2)	304	-
Tension strength, f_{frp} (MPa)	400	(ISO 10618)
Tensile modulus, E_f (GPa)	23	(ISO 10618)
Elongation (%)	1.7	(ISO 10618)
Thickness, t_f (mm)	0.167	-

2.3 Strengthening Schemes

Careful surface preparation was performed before attaching the composite material to the concrete surface. The aggregates in the concrete were revealed by sandblasting to create a rougher surface. Dust and other debris were then blown away using compressed air. After the surface was properly prepared, epoxy resin was mixed according to the manufacturer's guidelines. The epoxy resin coating was therefore applied to attach the CFRP strips to the concrete surface, and a plastic roller was used to press the resin through the fibers of the strips. Prepared CFRP strips are shown in Figure 2.

Before putting the RC deep beam bonded with CFRP strips through any kind of test, it needs to be cured at room temperature for a minimum of seven days in order to allow the epoxy resin to gain its maximum strength. Since the mechanical performance of the FRP composite/concrete interface is highly dependent on the quality of the FRP bonding process, all elements are carefully strengthened using the same methods. The strengthened region was covered in a u-shaped pattern with 50 mm wide

CFRP strips that were spaced 100 mm apart (center to center) and bonded together. CFRP had a thickness of 0.167 mm.

a) Mark the location of CFRP

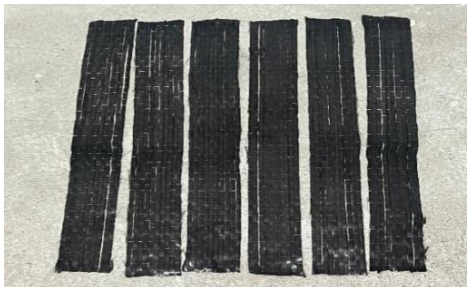

b) Cutting CFRP.

c) Mixing Resin Primer Coat

d) A layer of epoxy on the concrete surface.

e) Placing the CFRP over the concrete.

f) Final shape after CFRP strips strengthening from one side.

Figure 2: The procedure of CFRP strip strengthening technique

2.4 Instrumentation

All tests were performed on specimens loaded at all three points with a hydraulic jack with a capacity of 2500 kN in a self-supporting loading frame. The load was delivered at a rate of 1 kN/sec. Figure 3. Depicts a typical beam in the loading frame with several measuring devices and gauges; this configuration was utilized to conduct the beam test and gather the resulting data. To transmit the load and stop the concentration of strains, three bearing steel plates of constant width were put under the loading points and above the supports.

As can be seen in Figure 3. Linear variable displacement transducers (LVDTs) were installed under the beam's mid span to measure displacement throughout loading history. In addition, the two cameras were placed to read the load magnitude on the computer screen, while an excel sheet kept track of the deflection measurements as well as the strain in the concrete and steel. Figure 3. Shows this clearly.

Figure 3: Testing configuration of beam specimens

Table 4: summary of test result.

Group no.	Beams	H mm	Width of bearing plate (Bp) mm	f'_c mpa	First flexural cracking load, kN	First shear cracking load, kN	Ultimate load, kN	Ultimate Shear strength (MPa) $\frac{V_u}{b.d}$	Stress at first shear crack (MPa) $\frac{V_{cr}}{b.d}$	Normalized Ultimate load $\frac{V_u}{b.d\sqrt{f'_c}}$	**Shear strengthening%	*Increase in first racking load %	Failure mode
Group 1	1-W4-100	200	100	41.9	58	82	388	15.58	3.29	2.40		—	Strut crushing
	2-W2-100	400	100	41.9	103.8	215.6	586	11.29	4.15	1.70	—	—	Diagonal splitting
	3-W5 -100	600	100	41.9	204.1	304.7	718	8.83	3.74	1.36	—	—	Diagonal splitting
Group 2	4-W9-CFRP-100	200	100	32.9	75	108	385	15.46	4.33	2.7	12.5	29.31	Diagonal splitting +De-bonding
	5-W7-CFRP-100	400	100	32.9	145.6	279.7	622.9	12	5.38	2.09	22.94	40.2	Combined shear-compression +De-bonding

	6-W10-CFRP-100	600	100	32.9	276.4	414.7	955	11.74	5.1	2.04	50	35	Combined shear-compression +De-bonding

*Increase first cracking load% = $\frac{p_{cr\,(strengthened)} - p_{cr\,(refernce)}}{p_{cr\,(refernce)}} * 100$

** shear strengthening % = $\frac{v_{u,norm(strengthened)} - v_{u,norm(reference)}}{v_{u,norm(reference)}} * 100$

3.Test Results and Discussions

3.1 Cracking Behavior and Modes of Failure

A steady deformation of the specimens was seen as the applied load on the beams increased. Midspan deflection was continually recorded using an LVDT. The load at which the first shear crack developed on the beam surface was also recorded, and the specimens were inspected visually for any defects. In a similar procedure, beams' ultimate load-bearing capacity was measured at the locations where they collapsed and could no longer support any extra weight. All of the beams failed in shear. Flexural cracks appeared in the midspan area between 14.9% and 28.9% of the ultimate load and propagated to the beam's mid-depth. The diagonal crack first showed up between 21% and 44.9% of the maximum load and quickly propagated towards loading point and support.

The three types of failure seen in this research were shear-compression, Strut crushing, and diagonal splitting. The shear-compression failure may be identified from other types of failures by the crushing of the concrete that occurs above the upper end of the inclined crack. The connection between the struts and the load points failed due to a crushing strut failure. As the stress continued to build, many smaller, parallel inclined cracks emerged. Concrete between the fractures was destroyed, causing the structure to collapse. For the diagonal splitting mode to take place, there must be a crucial diagonal crack connecting the loading point and the support. Table 4. Provides an overview of the failure patterns seen across all of the tested specimens of beams in this investigation.

For the beams in the first group (1-W4-100, 2-W2-100, and 3-W5-100), there were three different overall depths (h). in 1-W4-100, 2-W2-100, and 3-W5-100 flexural cracks appeared in the specimen's pure bending region when the load was increased. Flexural cracks developed on the shear span between the loading point and support at 58 kN, 103.8 kN, and 204.1 kN, respectively, as load increased. Beam 1-W4-100, 2-W2-100, and 3-W5-100 all developed their initial shear cracks at loads of around 82 kN, 215.6 kN, and 304.7 KN, respectively. When the load was increased, more shear cracks formed, and the larger shear fractures moved upward along the beam. Figure 4. depicts the fracture pattern of group one, which includes beam specimens W4-100, W2-100, and W5-100, which failed at 388 kN, 586 kN, and 718 Kn with a mid-span deflection of 6.5 mm, 6.27 mm, and 4.1 mm, respectively.

Beams in group 2 (4-W9-CFRP-50, 5-W7-CFRP-100, and 6-W10-CFRP-150) are comparable to those in group 1 in terms of reinforcement details and geometric dimensions, but they are strengthened with

CFRP strips. CFRP sheets were applied in the shear zone, with the primary fiber direction perpendicular to the beam's longitudinal axis. Flexural cracks began showing up in the load-bearing center of the beams that lacked a CFRP covering. Initially, shear cracks showed themselves as CFRP sheet separation in beams 4-W9-CFRP-50, 5-W7-CFRP-100, and 6-W10-CFRP-150 at 108 kN, 279.7 kN, and 414.7 kN, respectively. Cracks in the beam's center area became taller as the loads were increased. As the loads were increased, the cracks in the beam's middle section spread upwards. The primary failure modes of the 4-W9-CFRP-100 beam were the tearing of the CFRP wrap and the debonding of the CFRP sheet at one end. In contrast, the 5-W7-CFRP-100 sample failed mostly due to the CFRP wrap separating and de-bonding, and the CFRP burst on either the first or second strip after being separated from the support. Beam 6-W10-CFRP-100 failed as a specimen due to cracking and debonding of the carbon fiber reinforcement (CFRP), peeling away of the concrete surface, and a rupture of the CFRP at the bottom beam's edge close to the support, as shown in Figure 5. For Crack Pattern for Group 2.

Figure 4: Crack patterns for beams of G1 at ultimate loads

Figure 5: Crack patterns for beams of G2 at ultimate loads

3.2 Load-Deflection Relationships

Midspan deflection was measured using a linear variable displacement transducer as a load was progressively applied during beam testing (LVDT). Midspan deflections were then plotted against loads. Midspan load-deflection curves for each beam specimens are shown in Figure 6&7. A beam's load-deflection relationship can be used to characterize the beam's response and ductility under stress. The first portion of any deflection curve is linear up to the appearance of fractures, especially inclined cracks; when the cracks appear, however, the second half of the curve is noticed, and it has become non-linear (inelastic behavior). In the non-linear region, the rate at which the deflection changes are greater than at the elastic stage. The deflection was raised before failure without the applied load changing. Each strengthened beam specimen had a greater starting stiffness than the control beams that were not strengthened. When comparing the un-strengthened sample to Figure 6, it is clear that the initial stiffness and the mid-span deflection both improve with increasing beam depth at a constant width of the bearing plate (1-W4-100, 2-W2-100, and 3-W5-100).

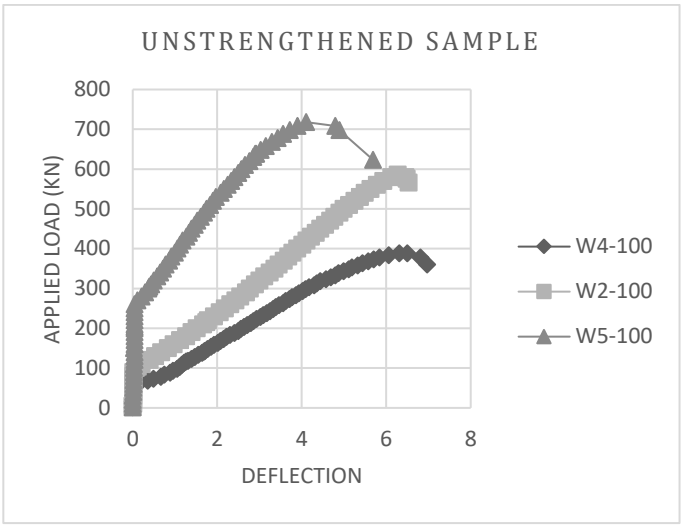

Figure 6: Load-deflection curves for unstrengthened specimens.

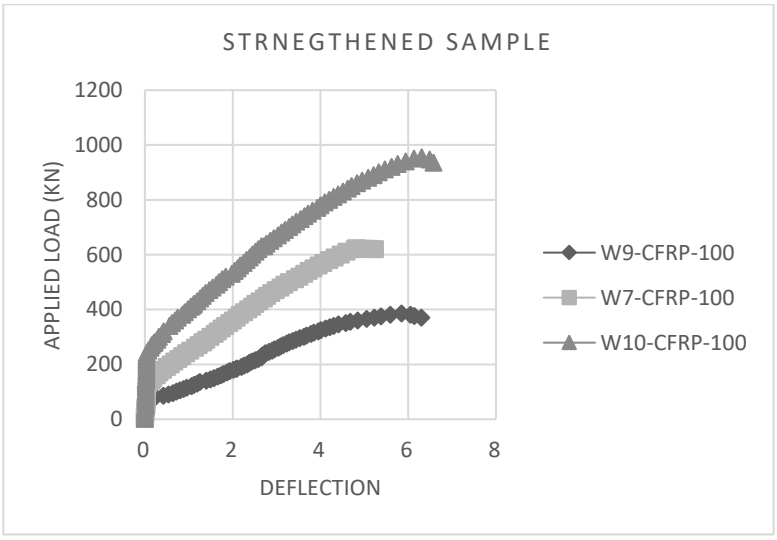

Figure 7: Continued, Load-deflection curves for strengthened specimens.

3.3 Cracking and Ultimate Strength

The cracking load is defined as the stress at which cracks first appeared in the specimen and began to propagate, indicating that the tensile stresses in the specimen had exceeded the capacity of the section. In this context, "ultimate load" refers to the utmost load that may be placed on the beam. Table 4 summarizes the ultimate and cracking loads for all specimens. Because test beams would inherently vary in compressive strength, we normalized the experimentally ultimate load concerning the concrete strength (V_(u,test)/b.d.√(f^' c)) to account for these discrepancies. In addition, Table 4 displays the normalization findings.

To understand the size effect on the shear strength of deep beams, Figure 8. plots the normalized shear strength at ultimate (V_(u,test)/b.d.√(f^' c)) against the height of the beams for groups 1 and 2. In the unstrengthened specimen, the shear strength decreased as beam height increased from 200 to 600 mm. In addition, the loss was much more apparent in strengthened samples. Figure 9. Is a graph depicting the relationship between the diagonal cracking strengths of Group 1 and Group 2 and the height of the

beam. It can be seen from this figure that Group 1 and Group 2 beams have nearly identical flat curves of diagonal cracking strength with beam height. This confirms the hypothesis that the strength of deep beams against diagonal cracking is independent of beam size. (Collins and Kuchma, 1999; Tan and Lu, 1999). However, the inclusion of carbon fiber reinforced plastic (CFRP) did affect the magnitude of diagonal cracking strength compared to unstrengthened specimens, with an increase of 47%, 46.8%, and 55%, respectively, for specimens with dimensions of 200mm, 400mm, and 600mm.

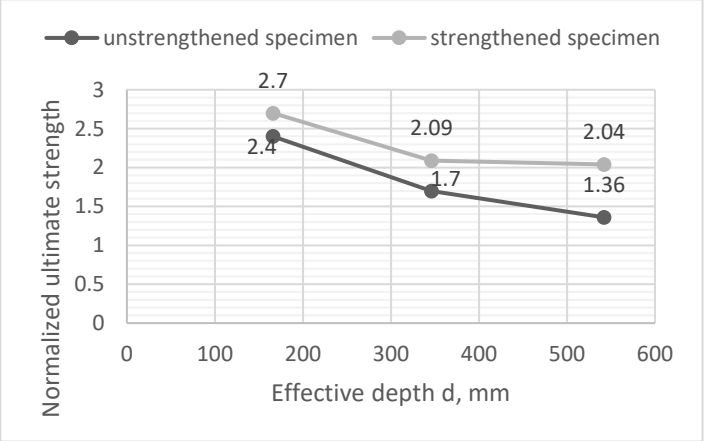

Figure 8: ultimate strength plotted against the effective depth of the beam.

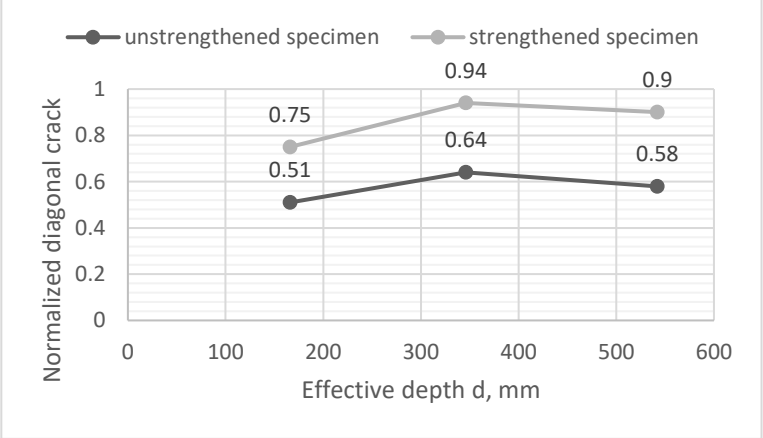

Figure 9: diagonal cracking strength plotted against the effective depth of the beam.

Figure 10 shows that the ultimate shear strength of the strengthened specimens increased by 12.5%, 22.94%, and 50% when compared to the control specimens of 200mm, 400mm, and 600mm, respectively.

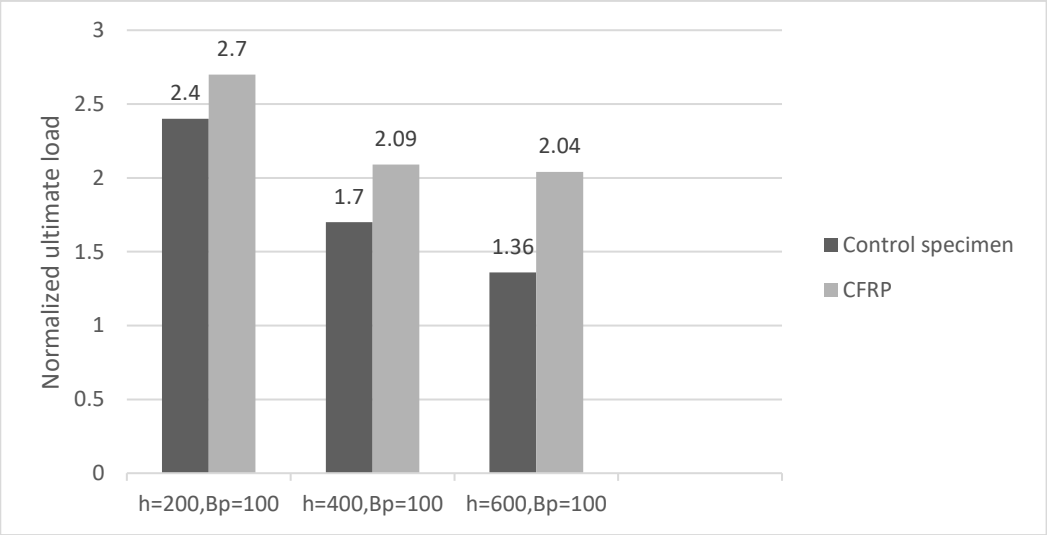

Figure 10: Normalized ultimate load as a function of beam size increases over all series.

4. Conclusion

This study reports the findings of an experimental program designed to determine how adding CFRP U-strips might affect the shear strength of RC deep beams. Additionally, the experimental program was designed to examine the effect of beam depth on final load-bearing capability and to refine the existing database. The specific findings of this study are summed up as follows, within the scope of the inquiry mentioned:

- A size effect was seen when the ultimate shear strength of a beam decreased with increasing beam height. An increase in height from 200 to 600 mm resulted in a 76% decrease in shear strength at ultimate.
- There is no size effect on the propagation rate of diagonal cracks in beams of varying sizes.
- The deep beams examined in this study that were strengthened in shear with CFRP u-strips exhibited an increase of around 12% to 50% compared to the comparable control beams.
- The presence of CFRP might influence the size effect of RC deep beams, with an increase in height from 200 to 600 mm resulting in a 32% decrease in the shear strength of strengthened specimens at ultimate.
- For the large-scale test beam, FRP strengthening was the most effective, but for the small-scale test beam, it was the least effective.
- The inclusion of CFRP did affect the magnitude of diagonal cracking strength, with increases of 47%, 46.8%, and 55% for specimens of 200mm, 400mm, and 600mm, respectively.
- The initial stiffness of all strengthened beam specimens is greater than that of their non-strengthened counterparts. The deflection of the control samples is larger than that of the strengthened samples.
- Initial stiffness improves with increasing beam size, and deflection decreases as beam size grow in unstrengthened specimens due to the size effect.

References

American Society for Testing and Material, A. C. (1996) ‘Standard Test Method for Splitting Tensile Strength of Cylindrical Concrete Specimens’.

Ashour, A. F. (1997) 'Tests of reinforced concrete continuous deep beams'. *Structural Journal*, 94(1), 3-12.

ASTM-A370-19 (2019) 'Standard Test Methods and Definitions for Mechanical Testing of Steel Products', 1-50.

Bae, S. W., Tann, B. D. and Belarbi, A. (2012) 'Size effect of reinforced concrete beams strengthened in shear with externally bonded CFRP sheets'. *Proceedings of the 6th International Conference on FRP Composites in Civil Engineering*, CICE 2012, 1-8.

Bazant, Z. P. K. M. T. (1991) 'Size effect of diagonal shear failure',". *ACI Struct. J*, 88 (3), 268-276.

Benzeguir, Z. E. A., El-Saikaly, G. and Chaallal, O. (2019) 'Size Effect in RC T-Beams Strengthened in Shear with Externally Bonded CFRP Sheets: Experimental Study', *Journal of Composites for Construction*, 23(6), 1-13. doi: 10.1061/(asce)cc.1943-5614.0000975.

Collins, M. P., and Kuchma, D. (1999) 'How safe are our large, lightly reinforced concrete beams, slabs, and footings?'. *Structural Journal*, 96(4), 482-490.

Committee, A. (2019) '318-19 Building Code Requirements for Structural Concrete and Commentary', 318-19 Building Code Requirements for Structural Concrete and Commentary. DOI: 10.14359/51716937.

Deniaud, C. and Cheng, J. (2001) 'Shear behavior of reinforced concrete strengthened with FRP sheets'. *Can. J. Civ. Eng*, 28(2), 271-281.

El-Sayed, A. K., and Shuraim, A. B. (2016) 'Size effect on shear resistance of high strength concrete deep beams', Materials and Structures/Materiaux et Constructions, 49(5), 1871-1882. DOI: 10.1617/s11527-015-0619-1.

Eurocode EN 12390-3 (2009) 'Testing hardened concrete', Part 3: Compressive Strength of Test Specimens.

Ghannoum, W. M. (1998) 'Size Effect On Shear Strength of Reinforced Concrete Beams', *M.S. thesis, Dept. of Civil Engineering and Applied Mechanics, McGill Univ.*

Godat, A. et al. (2010) 'Size Effects for Reinforced Concrete Beams Strengthened in Shear with CFRP Strips'. *Journal of Composites for Construction*, 14(3), 260-271. doi: 10.1061/(asce)cc.1943-5614.0000072.

Jumaa, G. B. and Yousif, A. R. (2019) 'Size Effect in Shear Failure of High Strength Concrete Beams without Stirrup reinforced with Basalt FRP Bars'. *KSCE Journal of Civil Engineering*, 23(4), 1636-1650. DOI: 10.1007/s12205-019-0121-3.

Kani, G. (1967) 'How safe are our large reinforced concrete beams?'. *in Proc. ACI J*, 64 (3), 128-141.

Khalifa, A. and Nanni, A. (2000) 'Improving shear capacity of existing RC T-section beams using CFRP composites'. *Cement and Concrete Composites*, 22(3), 165-174. doi: 10.1016/S0958-9465(99)00051-7.

Kim, G., Sim, J. and Oh, H. (2008) 'Shear strength of strengthened RC beams with FRPs in shear'. *Construction and Building Materials*, 22(6), 1261-1270. doi: 10.1016/j.conbuildmat.2007.01.021.

Leung, C. K. Y. et al. (2007) 'Effect of Size on the Failure of Geometrically Similar Concrete Beams Strengthened in Shear with FRP Strips'. *Journal of Composites for Construction*, 11(5), 487-496. doi: 10.1061/(asce)1090-0268(2007)11:5(487).

Long Nguyen-Minh, M. R. (2015) 'Size effect in uncracked and pre-cracked reinforced concrete beams shear-strengthened with composite jackets'. *Composites Part B*, 78, 361-376.

Qu, Z. and Lu, X. (2005) 'Size effect of shear contribution of externally bonded FRP U-jackets for RC beams', *Proceedings of International Symposium on Bond Behaviour of FRP in Structures (BBFS 2005)*, 371-380. Available at: http://www.luxinzheng.net/publication1/BFFS_size_effect.pdf.

Saribiyik, A., Abodan, B. and Balci, M. T. (2021) 'Experimental study on shear strengthening of RC beams with basalt FRP strips using different wrapping methods', *Engineering Science and Technology, an International Journal*, 24(1), 192-204. doi: 10.1016/j.jestch.2020.06.003.

Syroka-Korol, E. and Tejchman, J. (2014) 'Experimental investigations of size effect in reinforced concrete beams failing by shear'. *Engineering Structures*, 58, 63-78. doi: 10.1016/j.engstruct.2013.10.012.

Tan, K. H., and Lu, H. Y. (1999) 'Shear behavior of large reinforced concrete deep beams and code comparisons'. *ACI Structural Journal*, 96(5), 836-845. doi: 10.14359/738.

Triantafillou, T. C. and Antonopoulos, C. P. (2000) 'Design of Concrete Flexural Members Strengthened in Shear with FRP'. *Journal of Composites for Construction*, 4(4), 198-205. doi: 10.1061/(asce)1090-0268(2000)4:4(198).